COBEM 2023 27TH INTERNATIONAL CONGRESS OF MECHANICAL ENGENEERING

ABCM Brazilian Society of Mechanical Sciences and Engineering
27th ABCM International Congress of Mechanical Engineering
December 04-08, 2023, Florianópolis-SC, Brazil

COB-2023-1137
MASS REDUCTION AND MOBILITY IMPROVEMENT OF AN OVERHEAD POWERLINE INSPECTION ROBOT

Eduardo da Silveira de Meneses
Estevan Hideki Murai
Gustavo Queiroz Fernandes
Daniel Martins
Federal University of Santa Catarina. Campus Universitário Reitor João David Ferreira Lima, s/nº - Trindade, Florianópolis – SC, 88040-900
eduardosmeneses2001@gmail.com
estevan.murai@ufsc.br
gustavo.fernandes@posgrad.ufsc.br
daniel.martins@ufsc.br

Roberto Kinceler
Alessandro Pedro Dadam
Centrais Elétricas de Santa Catarina S.A. Av. Itamarati, 160 - Itacorubi, Florianópolis - SC, 88034-900
rkinceler@celesc.com.br
alessandropd@celesc.com.br

Abstract. *This paper focuses on the mass reduction and mobility improvement of an overhead power distribution line inspection robot to make it more technically and commercially feasible. The robot was designed by the Laboratory of Applied Robotics from the Federal University of Santa Catarina, in partnership with the public energy distribution service concessionaire of the state of Santa Catarina - Celesc, with the purpose of facilitating the electric distribution grid inspection. The inspection robot consists of a wheel with a shaft passing through its center; two compartments, one on each side of the wheel, connected to the central axis by pendulums, an anti-roll bar at the rear; and a gimbal fixed on top of the left compartment. The right compartment houses the motor and a set of pulleys to transmit the motion to the wheel. The left compartment contains the electronic components for the robot's operation. Both compartments guarantee the robot's center of mass is located below the contact point between its wheel and the power line aluminum conductors, maintaining its equilibrium passively. This paper presents changes implemented to the robot through the redesign of some of its subsystems, with the intention of reducing the robot's total mass and lowering its center of mass, thus improving obstacle transposition capability. Changes were made to the hubs, transmission pulley, and mainly to the pendulums and their compartments. The modifications resulted in an easier assembly process, a lower center of mass, and a greater equilibrium capacity than its previous version.*

Keywords: *Mass reduction, distribution line inspection robot, mobility improvement, design optimization, power lines inspection.*

1. INTRODUCTION

The uninterrupted supply of electric power is vital for sustaining the economic development and growth of urban centers. This growth causes an increase in the demand and consumption of electric energy, which requires an important network for its transmission and distribution (Gonçalves and Carvalho, 2014). In Brazil, the distribution of electricity from power substation facilities to end consumers is facilitated by an intricate network of overhead power distribution lines (OPDLs) spanning thousands of kilometers across diverse terrains, including densely populated cities, remote regions, and challenging natural landscapes.

Electric power distribution lines serve as the backbone of Brazil's electrical infrastructure, enabling the efficient and reliable distribution of electricity from power substations to consumers. With a rapidly expanding economy and an increasing reliance on electricity-intensive industries, the population requires a robust and extensive distribution grid to meet the nation's energy demands.

To guarantee the reliability and robustness of energy distribution, human operators are tasked with inspecting, diagnosing, and repairing OPDL components, often under challenging environmental conditions. Such maintenance operations require a high level of cognitive function and physical exertion. Furthermore, maintaining distribution lines presents inherent risks to human operators, including working at great heights, exposure to extreme weather conditions, and the potential for electrical hazards. These risks pose significant safety concerns and necessitate stringent safety

protocols and specialized training for personnel engaged in maintenance activities. The demanding workload can lead to fatigue, and delays in maintenance operations, making human inspections prone to misinterpretations and incorrect diagnosis, sometimes leading to inappropriate maintenance actions (Prates et al., 2019).

Given the challenges and limitations of human-led maintenance, the development and implementation of a distribution line inspection robot holds considerable promise. Robotics and automation technologies offer the potential to enhance safety, efficiency, and accuracy in distribution line maintenance. Robotic systems can operate in hazardous conditions, perform remote inspections, and gather real-time data, thus enabling proactive maintenance and minimizing downtime.

In this context, a partnership between the public energy distribution service concessionaire of the state of Santa Catarina (Celesc) and the Laboratory of Applied Robotics (LAR) from the Federal University of Santa Catarina (UFSC), designed an overhead distribution line inspection robot capable of moving and overcoming obstacles in OPDLs. To ensure the adequate performance of a robotic inspection system, key considerations include robust locomotion capabilities and sensor technologies for data acquisition.

During the robot development phase, a search for inspection robots for power lines was conducted; however, their configurations were not employed in this project due to their inability to meet certain requirements. Most of the robots found are for transmission lines and do not meet project requirements in terms of the robot`s mass and the nature of obstacles encountered. More aspects of the inspection robots found in the literature are shown by Brito et al. (2021b).

This article evaluates the mass reduction and mobility improvement of an overhead distribution powerline inspection robot. It is worth noticing that this robot construction was completed in 2021, and the robot was tested on a real distribution line. The robot rides above the aluminum conductor and it maintains its stability in a passive manner, *i.e.*, due to the pendulums, the robot's center of mass (C.M.) is below the contact point between the robot and the power line aluminum conductor. More details on the robot concept can be seen in de Brito et al. (2021a) and in Souza *et al.* (2022). The present article will focus on the project and analysis of possible modifications to make the robot lighter and more stable. Another issue observed for the robot developed in partnership with Celesc was the assembly complexity and lengthy time. Thus, during the components redesign, it was also considered how the components would be assembled after manufacturing. Therefore, in addition to reducing mass, another goal of this work was to make the replacement of parts simpler and to reduce the steps in the robot`s assembly process. In Section 2, the inspection robot design is briefly described. Section 3 shows the strategy adopted to reduce the robot's mass and lower its center of mass. Then, in Section 4 all modifications implemented on the robot are presented in comparison to its previous design. The findings reported earlier are deliberated upon in Section 5, wherein the enhancements implemented and potential future improvements are addressed. The conclusions are presented in Section 6.

2. ROBOT DESIGN

The inspection robot, shown in Fig. 1, is comprised of the following components: a thermal camera (A); a camera positioning and orientation system with two degrees of freedom (B); a wheel (C) with an axis passing through its center; a transmission system (D); photovoltaic cells to improve robot's autonomy (E), on-off user bottoms (F); a GPS antenna (G) to register the location of the OPDL faults; two compartments, one on each side of the wheel, connected by pendulums (H) to the central axis; and a stabilizing bar at the rear (not visible in Fig. 1). One of the compartments houses a DC motor, which is connected to a set of pulleys to transmit power to the wheel. The other compartment houses the electronic components necessary for the robot's operation. Both compartments ensure that the robot's center of mass is located below the point of contact between its wheel and the power line aluminum conductors, thus maintaining its balance passively.

Most of the robot's mass corresponds to structural components, batteries, cabling infrastructure, sensors and other electronic components, which are located at both compartments. Table 1 presents all robot subsystems, showing for each one of them, the quantity of manufactured and purchased components, its mass and its percentage mass .

When designing a distribution line inspection robot, it is necessary to consider the geometric constraints imposed by distribution lines. For this purpose, a specific distribution line has been chosen as a representative model for the robot's design. The model line has four different types of insulators and four different types of suspension insulators, all types with different geometry and dimensions. The insulators positions on the cross arm also vary, as illustrated in Fig. 2, which shows a 3-0 configuration (Fig. 2a), with all three insulators at one side of the pole, and a 1-2 configuration (Fig. 2b), with one insulator at one side of the pole and two at the other. Besides that, there are other line components, such as fuse cutouts, as well as environment elements, such rufous hornero nests, which act as obstacles for robot operation. More details on the model line and on its components can be seen in de Brito *et al.* (2021b) and Celesc (2014), respectively. Figure 2 also illustrates the most critical scenario on the model line regarding its limited space for the robot dimensions. As a result of these geometric constraints, lowering the robots' components to make the robot more stable can result in collisions with the distribution line components. On the other hand, adding a ballast to lower the robot's center of mass increases the total mass and the probability of aluminum conductor failure. The next section describes the strategy adopted to reduce the robot's mass, lower its C.M. and consequently improve its stability and mobility, while maintaining its overall dimensions.

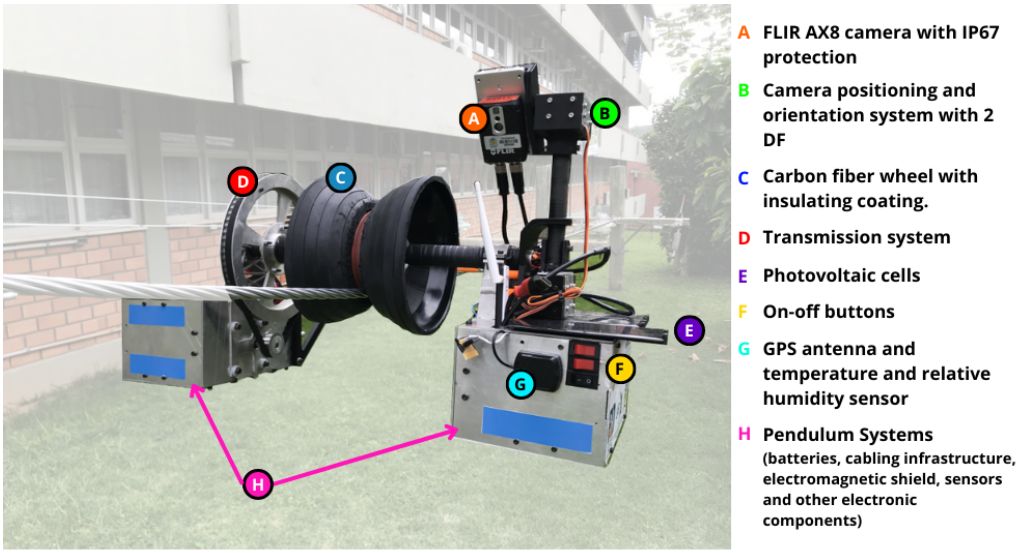

Figure 1. Inspection robot's main systems.

Table 1. Robot's subsystems and their masses

Subsystem	Total parts	Fabricated	Off-the-shelf	Mass (kg)	Mass (%)
Structure	67	16	51	3.466	28.35%
Batteries	19	0	19	2.281	18.65%
Transmission	22	9	13	1.723	14.10%
Motors e Controls	6	0	6	1.607	13.14%
Contact Superficies	8	4	4	0.887	7.25%
Electromagnetic Isolation	24	10	14	0.714	5.84%
Camera	25	13	12	0.596	4.87%
Cabling	4	0	4	0.440	3.60%
Sensors	12	3	9	0.433	3.54%
Processing and Communication	4	0	4	0.080	0.65%
TOTAL	**191**	**55**	**136**	**12.227**	

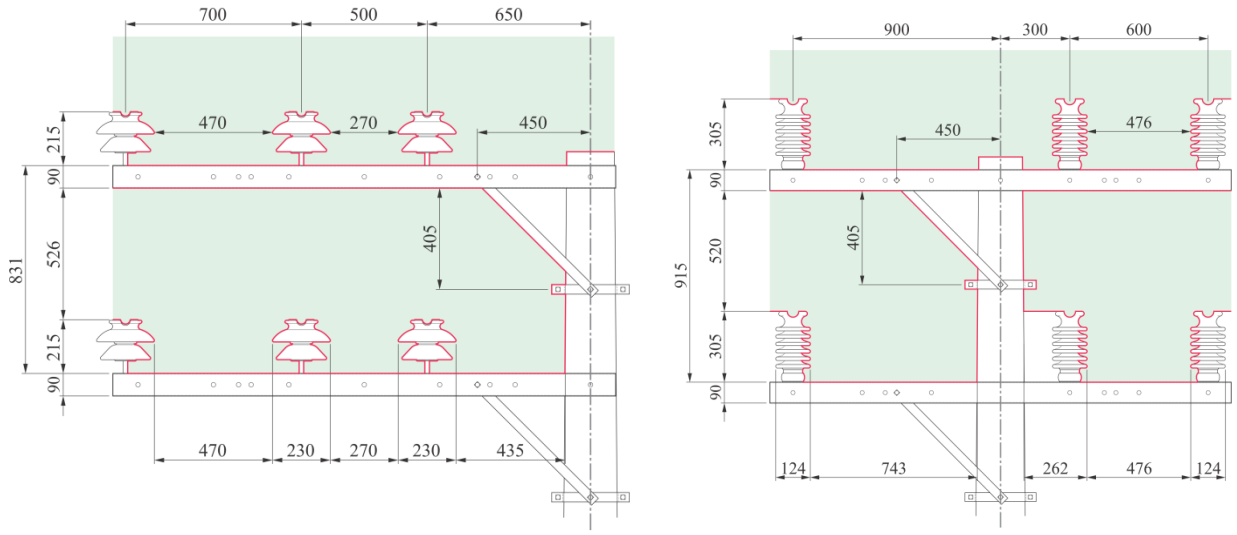

(a) (b)

Figure 2. Model line critical scenario for geometric delimitation. Adapted from de Brito *et al.* (2021b).

3. STRATEGY ADOPTED TO REDUCE MASS AND IMPROVE MOBILITY

Considering the information presented in the previous section regarding the robot's subsystems and their masses, the strategy employed to reduce the robot's mass and improve its mobility focused on selecting the subsystems and components with the largest mass for modification. Thus, mass was a first criterion used to prioritize the components to be modified.

The second criterion adopted was the center of mass. In this case, we focused on the subsystems which are above the contact point between the robot with the power line aluminum conductor. By doing so, the robot's center of mass is lowered, improving its capability to maintain its equilibrium passively.

Despite the robot's overall satisfactory performance, some components of the previously designed robot were not ideal for assembly and disassembly processes. Some components proved to be overly complex to assemble, mainly because of their excessive number of screws, difficult access to components, or extended assembly time. Therefore, a goal in this redesign process is to simplify the manufacturing, assembly and disassembly processes. Thus, a third criterion considered was to change components which present complex manufacturing or assembly processes.

As indicated in Tab. 1, the robot's structure has the highest contribution to the robot's total mass. Additionally, the project team reported several difficulties with this subsystem during the robot's assembly, especially regarding unnecessary components in the robot's compartments. Therefore the first modification considered improvements on the robot's structure, with the most significant elements analyzed being the external pendulum, the internal pendulum, and the compartments (Fig.3).

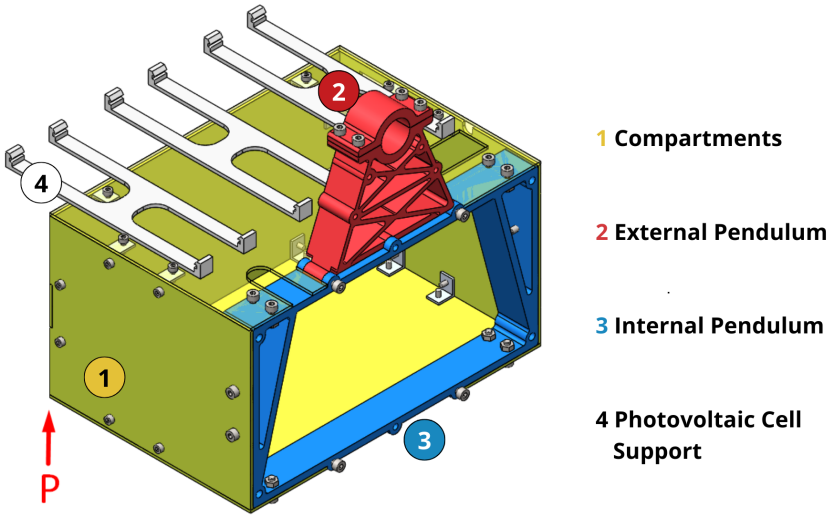

Figure 3. Elements of the robot's pendulum. Finite element analyses carried out for a load of 450 N at point P.

The internal structure and fittings of the external pendulum were modified after creating several CAD prototypes and carrying out finite element analyses (FEA) with them (Akin, 2010). For the FEA, it was considered a load of 450 N at point P (see Fig. 3). The load value was established considering the impact on the robot's structure during a fall from medium height. The analyses assumed this load could occur in any of the x, y or z directions, so that at least three different FEA analyses (one for each direction) were performed for each concept considered for the robot's pendulum. Based on the aforementioned changes, the internal pendulum was slightly modified to achieve a better fit within the compartments and with the external pendulum. Given that it is an essential part of the robot, various FEA were carried out on these structural components to verify the feasibility of these changes and thus ensure robot's integrity.

In sequence, despite not generating a significant change on the robot's total mass, the photovoltaic cells' support was redesigned to facilitate assembly and improve the cable management.

Next, the work focused on improving the transmission subsystem, which is the second subsystem with the greater mass. As illustrated in Fig. 4, the transmission subsystem is mainly composed of two hubs that hold together the mechanical elements that compose the robot wheel, a set of two pulleys to transmit power to the wheel and two plates connected to the greater pulley to guide the synchronous belt. The modifications included changes in the hubs concepts, reducing the number of screws that run through the wheel and hubs, and simplifying the assembly while still maintaining a proper coupling among the wheel components. Furthermore, the pulleys' mass was reduced through their

shortening and geometry modification. Once most components of the transmission subsystem are above the contact point to the aluminum conductor, these were some of the changes that impacted the most on lowering the robot's C.M. and improving its stability and mobility.

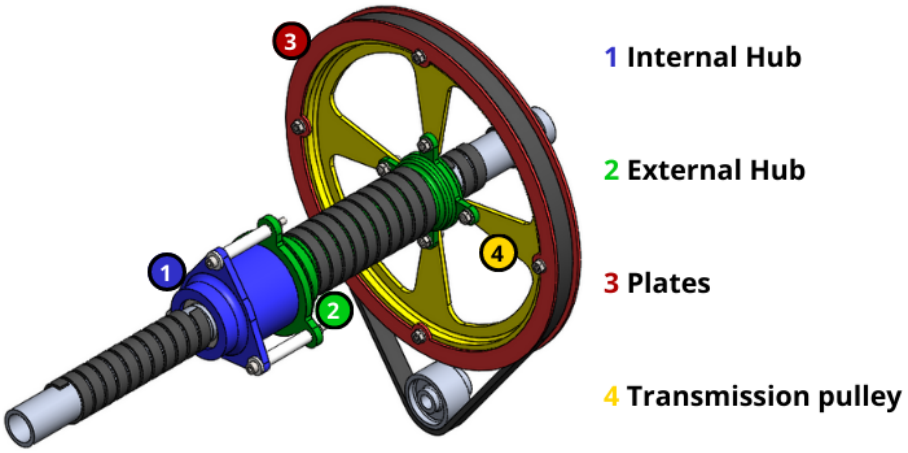

Figure 4. Components of the robot's transmission subsystem

Finally, the robot's camera and the positioning and orienting system (gimbal) were also changed. Initially, the robot used a FLIR AX8, a thermal and visual spectrum camera that has a mass of 125 g and requires a 180 g heat sink. As Fig.1 shows, the camera is above the aluminum conductor, raising the robot's center of mass. Thus, two lighter camera modules were chosen during the improvements, with equivalent technical specifications. The visual camera module, an OV2640 model, weighs 40g. The thermal camera module, FLIR Lepton 2.5, together with a FLIR Lepton® Breakout Board v2.0, has a mass of 0,9g. Changes on the gimbal considered moving the servo motors to within the compartments, avoiding extra insulation plates, and substituting the servo models from MG996R servos to micro 9G SG90 servos, which also meet the application torque requirements.

4. MODIFICATIONS

This section first addresses the conceptual changes pertaining to each modified component that constitutes the robot's structure. The structure subsystem plays a significant role in the robot's performance and any alteration in its configuration may have a substantial impact on the robot's mobility and balance, as well as on the robot's safety, integrity, and functionality. Consequently, the robot's structure has emerged as the first focus of the improvements described in this paper.

The first change occurred in the compartments (Fig. 5a). Instead of having an arrangement of six interconnected plates, the compartment was modified to two folded plates, a base and a cover. The portions of the base plate that come into contact with each other will be welded. The cover guarantees upper and lateral access to the components within the compartments, making the robot's assembly easier. This design was conceived with the aim of reducing the number of screws required during assembly and facilitating the handling of the components arranged within the compartments. In this case, the dimensions were maintained due to the decision to preserve the layout of the internal components. The compartments, considered in Aluminum 6063-T6 sheets of 2 mm thickness, reduced 66.49 grams, from 998.34 grams in its original design to 931.85 grams. after improvement.

In sequence, the study of possible changes shifted to the external pendulum (Fig. 5b) and internal pendulum (Fig. 5c) of the robot. As previously mentioned, numerous tests and analyses were conducted in the pursuit of discovering a configuration with a reduced mass that would effectively sustain the design loads from all three orientation axes, while remaining within the material's yield strength limit and avoiding significant displacement that could result in damage to the electronic components or structural rupture. Following this, it was determined that the width of 3mm of the external pendulum webs (Fig. 3) should be maintained while not changing the pendulum's material (Aluminum 7075-T6). However, the lower and central bars from the previous model were removed as they experienced minimal deformation when subjected to the 450 N loads. To lower stresses, fillets were added as highlighted in Fig. 6b (Budynas e Nisbett, 2011). These modifications resulted in a mass reduction of the component from 161.32 grams to 133.29 grams.

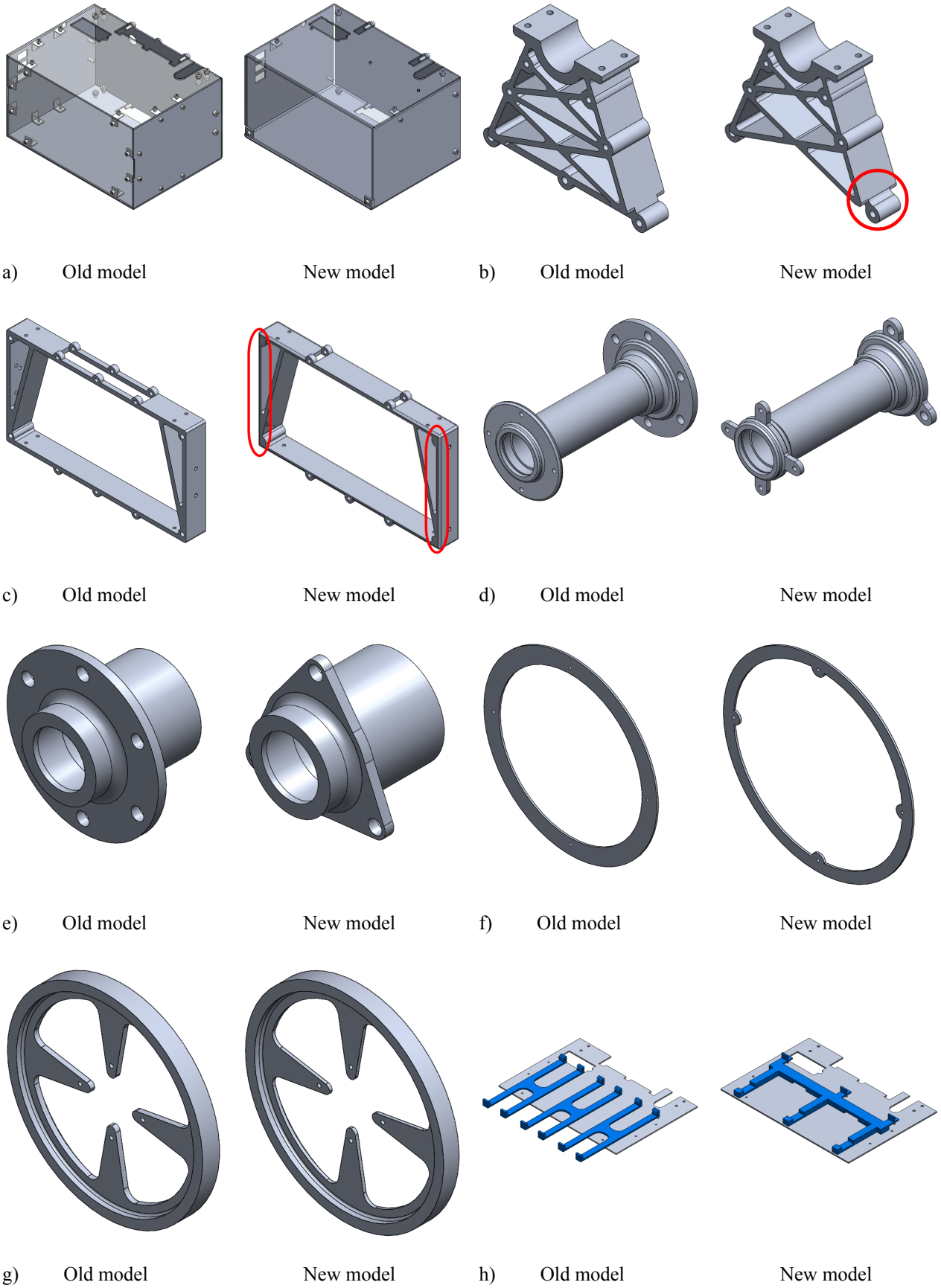

Figure 5. a) Compartments b) External Pendulum c) Internal Pendulum d) External Hub e) Internal Hub f) Transmission pulley g) Pulley guide plates h) Photovoltaic cells Support

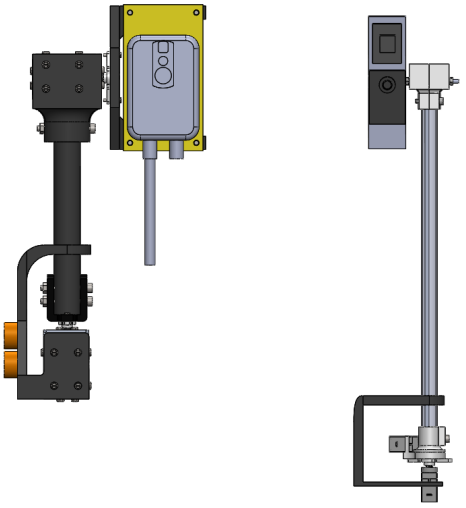

i) Old model New model

Figure 5 (continuation). i) Gimbal

The changes of the internal pendulum could not alter the internal dimensions of the compartments, which houses the robot's electronic devices, batteries and the DC motor. Increasing the compartment dimensions would also lead to collision to the OPDLs. Reduction of the internal pendulum's thickness also showed to increase considerably the tensions and displacements during the FEAs. Therefore, the changes to the internal pendulum were mostly rounding of the edges to achieve a better fit with the compartments, the elimination of several screw holes that will no longer be utilized in the design, and the sealing of the internal pendulum's upper opening, which has become unnecessary due to the modification of the external pendulum. Fillets were also added to lower stresses, as indicated in Fig. 5b. The aforementioned modifications resulted in a reduction of the component's mass from 308.83 grams to 273.00 grams.

As described in Section 3, FEA were carried out to guarantee the robot's integrity during modifications. The analyses considered a load of 450 N in *x*, *y*, or *z* directions, applied at a specific point as indicated in Fig. 3. Figure 6 shows the distribution of stress for each of these directions, considering the components of the compartments, the external pendulum and internal pendulum in their final improved version. The highest von Mises yield criterion at the internal and external pendulums occurs for the load in *z* direction (Fig. 6c) and is equal to 196 MPa. Simultaneously, the Aluminum 7075-T6 yield strength is equal to 503 MPa (Matweb, 2023a), suggesting the structure's integrity. Von Mises stresses higher than the yield strength of the Aluminum 6063-T6 (214 MPa) (Matweb, 2023b) used for the compartments were observed at the point of application of the 450 N only because this load is considered as concentrated at one point, what is not expected to occur in practical situations.

Next, the focus changed to the robot's transmission subsystem, which had a noteworthy opportunity for improvement in the internal hub (Fig. 5d). By altering the hub's design to incorporate three holes instead of six, and adopting a triangular shape that solely encompasses the retained apertures within the component, it becomes feasible to reduce both the mass and the number of screws traversing the piece. This modification will ease the assembly process while ensuring proper coupling of the wheel components. As a result of these adjustments, the mass of the internal hub decreased from 216.19 grams to 172.24 grams. Consequently, the external hub was compelled to have its fitting modified to accommodate only three holes as well (Fig. 5e). Furthermore, on the opposite end, instead of having diameters at the hub ends greater enough to encompass the screw holes, it was determined that the hub would have smaller diameter in its end and extend its radius merely on the regions necessary to encircle the four screw holes, thus reducing the amount of material. This adjustment resulted in a mass reduction of the external hub from 277.46 grams to 210.75 grams.

The concept of implementing a minor extension that merely circumvents the holes was also employed in the pulley guide plates (Fig. 5f); however, the alteration was not as drastic as in the case of the external hub so as not to compromise the integrity of the component. As a result of this modification, the pulley guide plates, which initially weighed 71.10 grams, were reduced to 47.85 grams.

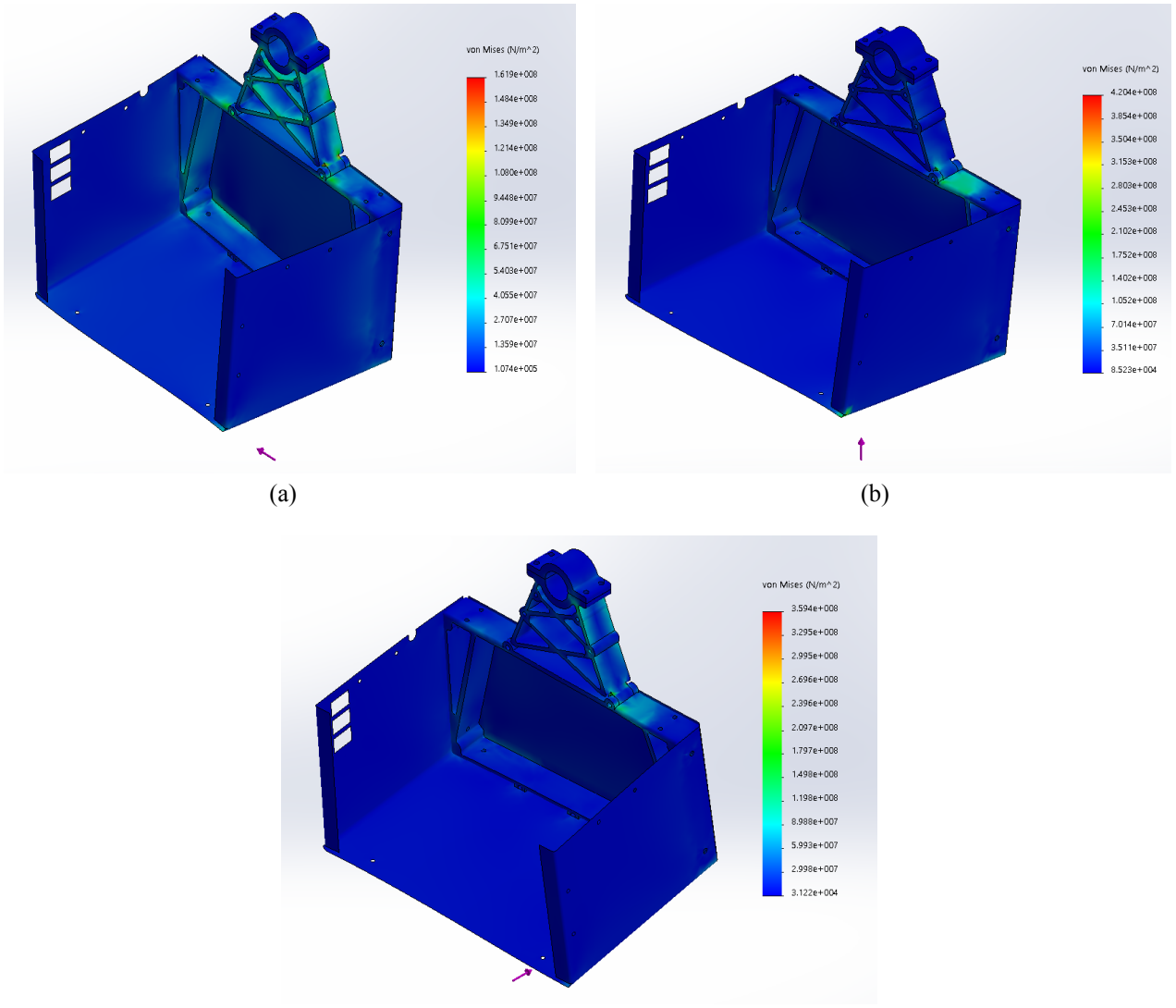

Figure 6. Finite element analysis considered a load of 450N in the x, y, and z directions, respectively.

Despite being the heaviest component of the transmission subsystem, the transmission pulley, also made of Aluminum 6063-T6, underwent a mere reduction in width from 19mm to 17mm (Fig. 5g). Nevertheless, this seemingly insignificant alteration resulted in a mass decrease from 484.74 grams to 390.94 grams.

Although it does not have significant relevance in the robot's mass, the photovoltaic cell support was completely modified (fig. 5h). What used to be three 3D-printed PLA pieces, glued to the upper surface of each of the two compartments, has now been replaced by a single piece that will support the cells. This piece will be securely attached to the surface using pins similar to those utilized in motherboards. This modification makes easier the connection of the photovoltaic cell cables to the DC grid and their removal during any maintenance.

Finally, after a brief analysis of the camera changes, which significantly contributed to the reduction in the subsystem's mass, it was identified as a good opportunity to redesign the support using a different concept than what was previously employed. The old gimbal (Fig. 5i) featured a larger and more robust support structure, with one servo located at the bottom responsible for rotating the camera on the vertical axis and another servo at the top responsible for rotating the camera on the horizontal axis, much like a typical gimbal system. Due to the gimbal's placement on top of one of the pendulum compartments (Fig. 1), both servos were exposed to the electromagnetic field generated by the transmission lines, requiring the use of small aluminum plates around both components, which added unnecessary mass to the overall subsystem. Moreover, a significant issue with the subsystem was the high number of screws used, which not only contributed to additional mass but also made the assembly process complex, taking over 5 hours to complete from scratch. As a solution, a new system was designed where both servos operate within the pendulum compartments,

eliminating electromagnetic interference and the need for aluminum plates around these two components. In this new concept (Fig. 5i), both servos are located at the bottom of the gimbal. However, the one responsible for the horizontal axis is assisted by a rod that moves up and down, thereby rotating the horizontal axis of the plate to which the cameras are attached. The assembly process was also rethought, using fewer screws and more interlocking or permanently attached parts. The team estimated that the assembly time for the new camera support prototype would be approximately 1 hour. The servos used were also changed, and while the gimbal of the old robot used two MG996R servo motors, the new robot has two 9G SG90 micro servos. As a result of this modification, the total mass of the gimbal was reduced from 969.57 grams to 172.12 grams.

5. DISCUSSION

Figure 7 illustrates the impact of the modifications described in this paper in the robot's C.M., which is directly related to the robot's passive equilibrium capacity. At the start of this work, the robot's initial C.M. was located 23.87 mm below the point the robot contacts the aluminum conductors. The improved C.M., represented in red, is now 37.81 mm below the contact to the conductors (a lowering of 13.94 mm in regard to the original C.M.). With this lowering on the robot`s C.M., it is expected an increase in robot stability, thus enhancing its safety. The impact of these modifications on robot performance will be evaluated practically in the future, as the next step of this work. The modifications described in this paper as well as other improvements already planned to the robot's design hold the potential to turn feasible one of the next project goals, which is to overcome larger and more complex obstacles. Furthermore, all components that underwent modifications experienced a reduction in their mass, thereby leading to a concomitant decrease in the robot's mass. The robot's initial mass of 12.227 kg has been reduced to 9.953 kg. Finally, the robot seems easier to assemble, with all components being redesigned in simpler ways, thereby reducing the number of assembly processes in the project. Table 2, summarizes the results of all the modifications described in this paper.

Table 2. Components mass comparison

Components	Old Model	New Model
Compartments	899.45 g	900.15 g
External Pendulum	161.32 g	133.29 g
Internal Pendulum	308.83 g	273.00 g
Internal Hub	216.19 g	182.24 g
External Hub	277.46 g	210.75 g
Plates	71.10 g	47.85 g
Transmission Pulley	484.74 g	390.94 g
Gimbal	969.57 g	172.12 g
Center of Mass	23.87 mm	37.81 mm
Total Mass	12.227 kg	9.953 kg

6. CONCLUSION

This study assessed the mass reduction and mobility improvement of an overhead powerline inspection robot. This improvement was achieved through conceptual modifications in the components of the subsystems with the highest contribution to the robot's total mass. Improvements on the assembly and disassembly processes and finite element analyses to guarantee robot's integrity during the modifications were also performed. Changes primarily involved a reduction in the quantity of utilized screws, removal of unnecessary structures, and alterations in thickness. Such modifications resulted not only in a decrease in the robot's total mass but also in the lowering of its center of mass, guaranteeing it more stability and enhancing its mobility.

As future works, the components housed within the pendulum compartments will be reorganized in an attempt to reduce robot's dimensions and lower even more its center of mass.. Future works also include the manufacturing and testing of a second robot prototype to practically evaluate the impact of the modifications described throughout this work on the robot's performance.

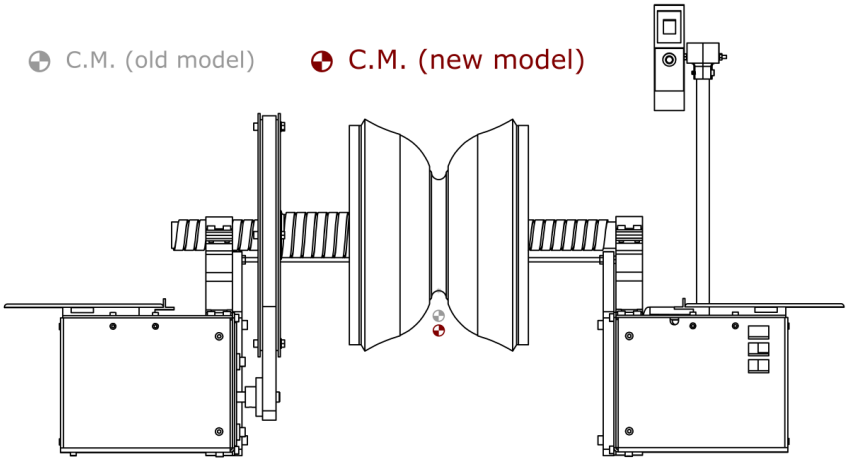

Figure 7. Visual comparison of the robot's center of mass before and after modifications.

7. ACKNOWLEDGEMENTS

This work was made as a continuation of the R&D project entitled "Development of a Robotized System for Inspection of Electricity Distribution Lines" (05697-0317 / 2017), regulated by ANEEL and financed by Centrais Elétricas de Santa Catarina (Celesc). The project is executed at the Laboratory of Applied Robotics (LAR), at UFSC, and financially managed by FEESC. The authors also thank CNPq and CAPES for the financial support.

8. REFERENCES

Akin, J. E., 2010. "Finite Element Analysis Concepts: Via SolidWorks" 1.ed. World Scientific. 335p.

Alhassan, A. B., Zhang, X., Shen, H., Xu, H.: Power transmission line inspection robots: A review, trends and challenges for future research. International Journal of Electrical Power & Energy Systems, v.118, p. 105862, Elsevier, (2020).

Budynas, R. G., Nisbett, J. K., 2011. "Elementos de Máquinas de Shigley: projeto de engenharia mecânica". 8. ed. São Paulo: Amgh. 1084 p.

Celesc, 2014. "E-313.0002: Estruturas para redes aéreas convencionais de distribuição".

de Brito, J. V. F., Murai, E. H., Fernandes, G. Q., Pereira, R. A. A., Martins, D., Kinceler, R., Dadam, A. P., 2021a. "Static equilibrium analysis of a distribution line riding robot with passive balancing system.". In *Proceedings of the 26th International Congress of Mechanical Engineering - COBEM 2021*. Florianópolis, Brazil.

de Brito, J. V. F., Murai, E. H., Fernandes, G. Q., Pereira, R. A. A., Martins, D., Kinceler, R., Dadam, A. P., 2021b. "Static equilibrium analysis of a distribution line riding robot with active balancing system.". In *Proceedings of the 26th International Congress of Mechanical Engineering - COBEM 2021*. Florianópolis, Brazil.

MatWeb, 2023a. "The Online Materials Information Resource - Aluminum 7075-T6; 7075-T651". Disponível em: <https://www.matweb.com/search/DataSheet.aspx?MatGUID=4f19a42be94546b686bbf43f79c51b7d>. Acesso em 10 de julho de 2023.

MatWeb, 2023b. "Matweb - The Online Materials Information Resource - Aluminum 6063-T6". Disponível em: <https://www.matweb.com/search/DataSheet.aspx?MatGUID=333b3a557aeb49b2b17266558e5d0dc0>. Acesso em 10 de julho de 2023.

Prates, R. M., Cruz, R., Marotta, A. P., Ramos, R. P., Simas Filho, E. F., Cardoso, J. S., 2019. "Insulator visual nonconformity detection in overhead power distribution lines using deep learning". Computers & Electrical Engineering, Vol. 78, pp. 343–355.

Souza, M. B., Meneghini, L., Artmann, V. N., Pinto, J. R. R., Murai, E. H., Martins, D., Kinceler, R., 2022. "Conceptual Design of an Inspection Robot for Distribution Power Lines that Moves on the Cables". In *Proceedings of the XIV Latin-American Congress on Electricity Generation and Transmission - CLAGTEE 2022*. Rio de Janeiro, Brazil.

Toussaint, K., Pouliot, N., Montambault, S.: Transmission line maintenance robots capable of crossing obstacles: state-of-the-art review and challenges ahead. Journal of Field Robotics, v. 26, n.5, pp.477–499 (2009). doi:10.1002/rob.20295.

9. RESPONSIBILITY NOTICE

The authors are the only responsible for the printed material included in this paper.